Cancer Cell
Article

A Cullin3-KLHL20 Ubiquitin Ligase-Dependent Pathway Targets PML to Potentiate HIF-1 Signaling and Prostate Cancer Progression

Wei-Chien Yuan,[1,2,11] Yu-Ru Lee,[1,3,11] Shiu-Feng Huang,[4,5] Yu-Min Lin,[1,2] Tzu-Yin Chen,[1,2] Hsiang-Ching Chung,[1,2] Chin-Hsien Tsai,[2,6] Hsin-Yi Chen,[1] Cheng-Ta Chiang,[1,2] Chun-Kai Lai,[1,2] Li-Ting Lu,[1,2] Chun-Hau Chen,[7] De-Leung Gu,[8,9] Yeong-Shiau Pu,[10] Yuh-Shan Jou,[8] Kun Ping Lu,[7] Pei-Wen Hsiao,[6] Hsiu-Ming Shih,[8] and Ruey-Hwa Chen[1,2,3,*]
[1]Institute of Biological Chemistry, Academia Sinica, Taipei, Taiwan
[2]Institute of Biochemical Sciences, College of Life Science
[3]Institute of Molecular Medicine, College of Medicine
National Taiwan University, Taipei, Taiwan
[4]Division of Molecular and Genomic Medicine, National Health Research Institutes, Zhunan, Taiwan
[5]Department of Pathology, Chang Gung Memorial Hospital, Tao Yuan, Taiwan
[6]Agricultural Biotechnology Research Center, Academia Sinica, Taipei, Taiwan
[7]Cancer Biology Program and Biology of Aging Program, Department of Medicine, Beth Israel Deaconess Medical Center, Harvard Medical School, Boston, MA, USA
[8]Institute of Biomedical Sciences, Academia Sinica, Taipei, Taiwan
[9]Institute of Microbiology and Immunology, School of Life Science, National Yang Ming University, Taipei, Taiwan
[10]Department of Urology, National Taiwan University Hospital, Taipei, Taiwan
[11]These authors contributed equally to this work
*Correspondence: rhchen@gate.sinica.edu.tw
DOI 10.1016/j.ccr.2011.07.008

SUMMARY

Tumor hypoxia is associated with disease progression and treatment failure, but the hypoxia signaling mechanism is not fully understood. Here, we show that KLHL20, a Cullin3 (Cul3) substrate adaptor induced by HIF-1, coordinates with the actions of CDK1/2 and Pin1 to mediate hypoxia-induced PML proteasomal degradation. Furthermore, this PML destruction pathway participates in a feedback mechanism to maximize HIF-1α induction, thereby potentiating multiple tumor hypoxia responses, including metabolic reprogramming, epithelial-mesenchymal transition, migration, tumor growth, angiogenesis, and chemoresistance. In human prostate cancer, overexpression of HIF-1α, KLHL20, and Pin1 correlates with PML down-regulation, and hyperactivation of the PML destruction pathway is associated with disease progression. Our study indicates that the KLHL20-mediated PML degradation and HIF-1α autoregulation play key roles in tumor progression.

INTRODUCTION

Hypoxia is an essential feature of the microenvironment of solid tumors. A key mechanism mediating the adaptation of hypoxia is the induction of hypoxia-inducible factor 1 (HIF-1). This transcription factor regulates a large panel of genes that play crucial roles in many aspects of cancer biology, including immortalization, stem cell maintenance, autocrine growth, metabolic reprogramming, angiogenesis, invasion, metastasis, and resistance to therapy (Brahimi-Horn et al., 2007; Finger and Giaccia, 2010; Semenza, 2010). Accordingly, accumulation of HIF-1 in solid tumors is associated with poorer patient prognosis and

Significance

Tumor hypoxia and HIF-1 play central roles in disease progression and treatment failure. Herein, we describe a PML destruction pathway mediated by the coordinated actions of Cul3-KLHL20, CDK1/2, and Pin1 and demonstrate that this pathway participates in a feedback mechanism to maximize HIF-1 induction. As a result, this PML destruction pathway promotes multiple tumor hypoxia responses, including metabolic reprogramming, EMT, migration, tumor growth, angiogenesis, and chemoresistance. More importantly, we show the existence of this pathway in human prostate cancer and its hyperactivation correlates with high-grade tumor. Our study identifies biomarkers that predict poor prognosis and provides mechanistic insights into the aggressive behaviors of high-grade tumors. Targeting components of this pathway may potentially be effective in treatment of aggressive prostate tumors.

more-aggressive tumor phenotypes (Brahimi-Horn et al., 2007). HIF-1 is therefore considered as an attractive target for pharmaceutical intervention in cancer therapy.

HIF-1 is a heterodimeric protein composed of a tightly regulated α subunit and a constitutively expressed β subunit (Wang et al., 1995). The α subunit is subject to ubiquitin-mediated proteolysis through an O_2-dependent pathway and is stabilized under hypoxia (Maxwell et al., 1999). In addition to this pathway, the level and/or activity of HIF-1α are also controlled by a complex network of positive and negative feedback regulators (Henze and Acker, 2010). This intricate HIF-1α regulatory system allows tumor cells to flexibly adjust and adapt hypoxia responses to the diverse and fluctuating oxygen concentrations within the tumor microenvironment, thereby benefiting tumor progression. However, the regulatory network of HIF-1α and its signaling mechanism in cancer cells have not been completely characterized, and a better understanding of these aspects may be beneficial for cancer therapy.

Besides hypoxia, HIF-1α protein level can be up-regulated in cancer by loss of function of several tumor suppressors (Semenza, 2010), including the promyelocytic leukemia (PML) protein (Bernardi et al., 2006). The *PML* gene was identified at the breakpoint of the t(15; 17) chromosome translocations of acute promyelocytic leukemia, which results in the generation of oncogenic PML-RARα fusion protein (de Thé et al., 1990; de Thé et al., 1991; Melnick and Licht, 1999). The PML protein is essential for the assembly of discrete subnuclear structures called PML-nuclear bodies (PML-NBs) (Ishov et al., 1999) and plays a critical role in multiple cellular processes that are altered in cancer, such as proliferation, apoptosis, senescence, migration, and angiogenesis (Bernardi and Pandolfi, 2007; Reineke et al., 2010; Salomoni et al., 2008; Salomoni and Pandolfi, 2002). In addition, PML loss sensitizes mice to tumorigenesis induced by physical or chemical carcinogens (Wang et al., 1998) and accelerates tumor onset in several mouse cancer models (Scaglioni et al., 2006; Trotman et al., 2006). In accordance with its tumor suppressive role, down-regulation of PML protein is frequently observed in diverse types of human tumors and is correlated with tumor progression. Because *PML* transcripts do not display a corresponding decrease, it has been proposed that PML protein is aberrantly degraded in tumors (Gurrieri et al., 2004; Salomoni et al., 2008).

PML protein degradation can be triggered by several signaling pathways. For instance, As_2O_3-induced PML sumoylation facilitates its ubiquitination by ubiquitin ligase RNF4, thereby inducing PML degradation (Lallemand-Breitenbach et al., 2008; Tatham et al., 2008). PML phosphorylation by CK2 results in its ubiquitination and degradation (Scaglioni et al., 2006). The peptidyl-prolyl *cis/trans* isomerase Pin1 (Reineke et al., 2008) and ubiquitin ligases Siah (Fanelli et al., 2004) and E6AP (Louria-Hayon et al., 2009) also act on PML to trigger its degradation. Although several signals and molecules promote PML ubiquitination and/or degradation, their contribution to frequent PML down-regulation in human tumors remains largely unexplored.

Many BTB domain-containing proteins serve as substrate adaptors in Cullin 3 (Cul3)–based ubiquitin ligases (Pintard et al., 2004). We previously identified that the BTB family protein KLHL20 forms an E3 ligase complex with Cul3 and Roc1 and a portion of KLHL20 exists in PML-NBs (Lee et al., 2010). In this study, we investigated how KLHL20 regulates the abundance of PML and the impact of this regulation on tumor hypoxia responses.

RESULTS

Hypoxia Induces PML Destabilization and *KLHL20* Transcription Through HIF-1

Hypoxia is known to regulate the expression of a number of genes responsible for tumor progression. We tested whether hypoxic stress influences the expression of PML. Hypoxia treatment of prostate cancer cell lines LNCaP and PC3 led to a time-dependent reduction of PML protein (Figure 1A) but not *PML* mRNA (see Figure S1A available online). Most, if not all, PML isoforms detected in these cell lines were affected by hypoxia. This hypoxia-induced PML down-regulation was observed in several other cancer cell lines, such as CWR22Rv1 (prostate), T47D (breast), H630 (colon), HCT116 (colon), and H1299 (lung) (Figure S1B). Cycloheximide-chase experiment revealed that hypoxia accelerated PML protein turnover (Figure 1B) by reducing $t_{1/2}$ from 6 hr to 1.6 hr. Furthermore, proteasome inhibitor MG132 triggered a greater PML up-regulation in hypoxic than normoxic cells (Figure 1C), supporting an involvement of the 26S proteasome. Protein degradation through proteasome usually results from polyubiquitin modification. We therefore examined PML ubiquitination level. Using LNCaP cells expressing PML-I, the longest and most abundantly expressed isoform of PML (Condemine et al., 2006), we found that PML-I polyubiquitination level was greatly elevated by hypoxia, as determined by reciprocal precipitation for either PML-I or ubiquitin (Figure 1D; Figure S1C). These results indicate that hypoxia induces PML polyubiquitination, which in turn triggers its proteasomal-dependent degradation.

Recent studies indicated that PML SUMO-2/3 conjugation promotes its ubiquitination by recruitment of the ubiquitin ligase RNF4 (Lallemand-Breitenbach et al., 2008; Tatham et al., 2008). To investigate whether hypoxia-induced PML ubiquitination was triggered by its sumoylation, we utilized a sumoylation-defective mutant PML-I 3KR (Figure S1D). Surprisingly, under hypoxia conditions, this mutant was ubiquitinated and degraded to similar extents as compared with the wild-type protein (Figure 1D; Figures S1C and S1E), indicating the existence of a sumoylation-independent mechanism.

Our recent study revealed that KLHL20 functions as a substrate adaptor of Cul3-based ubiquitin ligase and that a portion of KLHL20 is localized in PML-NBs (Lee et al., 2010). In agreement with a previous report (Nacak et al., 2007), hypoxia led to the up-regulation of *KLHL20* mRNA (Figure S1F) and protein (Figure 1A). Overexpression of HIF-1α(△ODD), a nondegradable mutant of HIF-1α, similarly induced KLHL20 (Figure S1G). Importantly, in both conditions, the increase of KLHL20 was correlated with a decrease of PML expression. The expression of RNF4, however, was unchanged (Figure 1A; Figure S1G). In the reciprocal experiment, HIF-1α depletion blocked hypoxia-induced up-regulation of KLHL20 and down-regulation of PML (Figure 1E), further demonstrating opposite regulations of the two proteins. To determine the mechanism by which HIF-1α regulates KLHL20, we identified two putative hypoxia-responsive elements (HREs) in promoter and intron 1

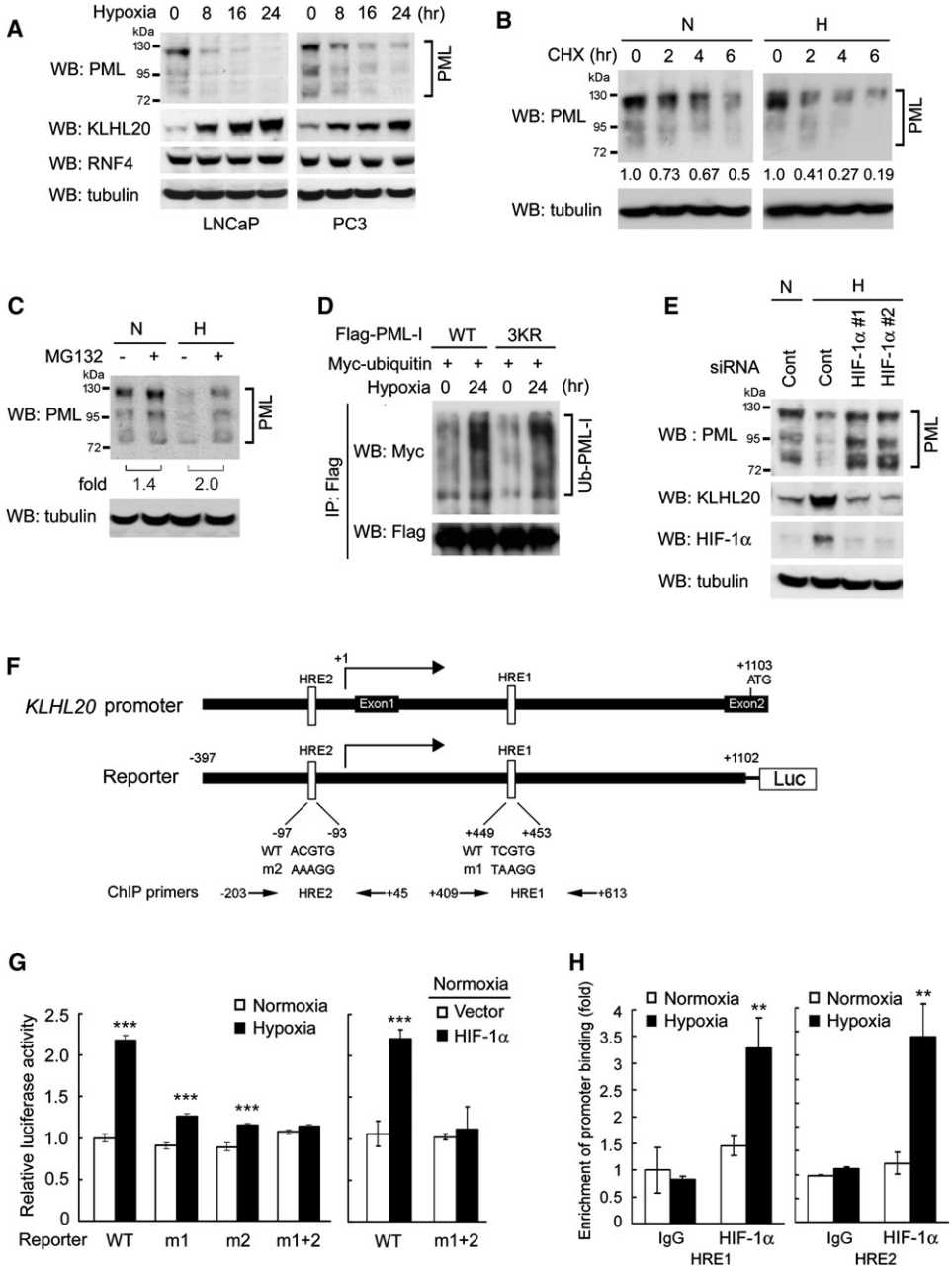

Figure 1. Hypoxia Induces Opposite Regulations of PML and KLHL20 through HIF-1α

(A) The expression of endogenous PML, KLHL20, and RNF4 in PC3 and LNCaP cells treated with hypoxia for indicated period.

(B and C) Western blot analysis of PML level in LNCaP cells cultured in normoxia (N) or hypoxia (H) and treated with cycloheximide (CHX) for indicated time points (B) or MG132 for 16 hr (C). The amounts of PML relative to that in untreated cells (B) and the fold of increase in PML level (C) are indicated.

(D) Hypoxia promotes PML ubiquitination independently of its sumoylation. LNCaP cells transfected with indicated constructs were cultured in normoxia or hypoxia for 24 hr. Cells were harvested for immunoprecipitation and western blot analyses with indicated antibodies.

(E) HIF-1α mediates hypoxia-induced PML down-regulation and KLHL20 up-regulation. PC3 cells infected with lentivirus carrying control or HIF-1α siRNA were cultured in normoxia or hypoxia for 24 hr and were assayed for western blot with indicated antibodies.

(F) Schematic representations of the regulatory region of *KLHL20* gene, the luciferase reporter constructs, and the ChIP primers used in this study. The positions of HREs and the sequences of wild-type and mutant HREs are indicated.

(G) Promoter activity assay using PC3 cells transfected with indicated reporter construct and HIF-1α and cultured in normoxia or hypoxia for 6 hr.

(H) qChIP assay of PC3 cells cultured in normoxia or hypoxia for 6 hr. Results in (G) and (H) are presented as mean ± SD (**p < 0.005, ***p < 0.0005, n = 3).

See also Figure S1.

of the *KLHL20* gene, respectively (Figure 1F). Mutation of either HRE reduced, and that of both HREs abolished, the hypoxia- or HIF-1α-induced *KLHL20* promoter activity (Figure 1G). Chromatin immunoprecipitation (ChIP) analysis confirmed the direct binding of HIF-1α to these *KLHL20*-regulating regions, and such binding was abrogated in cells expressing HIF-1α siRNAs (Figure 1H; Figure S1H). Furthermore, by mining through public gene expression databases, we revealed the coordinated up-regulation of *KLHL20* and a number of HIF-1 and/or HIF-2 targets in a cohort of colon cancer specimens, as compared with normal colon tissues (Figure S1I). Together, our results indicate that HIF-1 directly regulates *KLHL20* transcription and that KLHL20 induction correlates with PML destabilization in response to hypoxia.

Cul3-KLHL20 Ubiquitin Ligase Is Responsible for PML Ubiquitination

The opposite regulations of KLHL20 and PML suggest that PML is a substrate of the KLHL20-Cul3 ligase. As reported previously (Lee et al., 2010), KLHL20 was partially localized in PML-NBs in normoxia. During hypoxia, the KLHL20 immunofluorescent intensities in NBs and nucleus were both elevated (Figure S2A), correlating with the increase of total KLHL20 level. Cul3 was more concentrated in the nucleus than in the cytoplasm, especially under hypoxia conditions (Figure S2B). These subcellular distributions support the action of KLHL20-Cul3 complex on PML. In line with this notion, we detected the endogenous interaction between PML and KLHL20 (Figure 2A). More importantly, knockdown of KLHL20 by two different siRNAs abrogated hypoxia-induced PML down-regulation, whereas knockdown of RNF4 to a similar extent only slightly increased PML level in hypoxic cells (Figure 2B). This KLHL20 siRNA-induced PML accumulation in hypoxic cells was correlated with an increase of PML-NBs (Figure 2C). Notably, KLHL20 depletion also moderately up-regulated PML in normoxic cells (Figure 2B), consistent with a low but detectable amount of KLHL20 in such conditions. In keeping with these findings, PML-I ubiquitination was down-regulated drastically in hypoxic and moderately in normoxic cells by KLHL20 siRNA (Figure 2D). Conversely, PML-I ubiquitination was moderately increased by KLHL20 overexpression and drastically elevated by coexpression of KLHL20 and Cul3 (Figure 2E). KLHL20m6, which is defective in Cul3 binding (Lee et al., 2010), failed to induce PML-I ubiquitination. The kelch domain deletion mutant KLHL20△K also could not confer PML-I ubiquitination (Figure S2C), consistent with a role of this domain in substrate recruitment (Pintard et al., 2004). However, the PML-I 3KR was ubiquitinated at a level similar to wild-type protein by Cul3-KLHL20, indicating that sumoylation is dispensable for this ubiquitination event. Cul3-KLHL20 also promoted the ubiquitination of another PML isoform, PML-IV (Figure S2D). Furthermore, overexpression of KLHL20, but not KLHL20m6, promoted the turnover of PML-I and PML-IV (Figures S2E and S2F) and reduced the abundance of most, if not all, PML isoforms through a proteasome-dependent manner (Figure S2G). These data indicate a critical role of Cul3-KLHL20 complex in promoting the ubiquitination of most PML isoforms and in mediating hypoxia-induced PML down-regulation.

In contrast to the drastic down-regulation of PML protein, the number and size of PML-NBs were only modestly reduced in response to hypoxia (Figures S2H and S2I). Because PML sumoylation and interaction with SUMO-conjugated proteins are essential for NB assembly (Lin et al., 2006), we investigated these aspects in hypoxic cells. Remarkably, hypoxia induced PML SUMO-1 conjugation (Figure S2J, left), which likely results from reactive oxygen species–stimulated PML oligomerization/sumoylation (Jeanne et al., 2010) and a global up-regulation of protein SUMO-1 conjugation (Figure S2J, right). These phenomena were accompanied by an increased interaction of PML with Daxx, a PML partner in NBs. These data support a role of hypoxia in stimulating PML-NB assembly through a SUMO-dependent recruitment of NB-residing proteins, which is expected to alleviate the negative regulation of PML-NBs caused by hypoxia-induced PML degradation.

To address a direct role of Cul3-KLHL20 in PML ubiquitination, in vitro ubiquitination assay was performed. Incubation of purified PML-I with the KLHL20-Cul3-Roc1 complex in the in vitro ubiquitination reaction resulted in PML-I polyubiquitination. Omission of the E1, E2, or E3 ligase complex and replacement of Cul3 with a Roc1 binding-defective mutant (Cul3△C) or replacement of KLHL20 with KLHL20m6 abolished PML-I ubiquitination (Figure 2F). Furthermore, treatment of purified PML-I with calf intestine phosphatase (CIP) abrogated PML-I ubiquitination by KLHL20-Cul3-Roc1 complex. These data indicate that PML is a direct substrate of Cul3-KLHL20 ubiquitin ligase. However, targeting PML to this ligase requires a phosphorylation event.

CDK1 and CDK2 Phosphorylate PML S518 to Promote KLHL20-Mediated PML Destruction

To identify the kinase responsible for targeting PML to KLHL20, we screened a panel of kinase inhibitors. For simplicity, KLHL20 overexpression was used to mimic the effect of hypoxia. Among these inhibitors, only the pan-CDK inhibitor roscovitine blocked KLHL20-induced degradation of PML-I, whereas a CDK4/6-specific inhibitor failed to do so (Figure S3A). Roscovitine also blocked KLHL20-induced degradation of endogenous PML (Figure 3A) and Cul3-KLHL20-induced PML-I ubiquitination (Figure S3B). Furthermore, dominant negative (DN) mutant of CDK1 or CDK2, but not CDK4 or CDK6, abrogated KLHL20-induced PML-I degradation (Figure 3B). Consistent with these findings, in serum-starved, G1-arrested cells, which should be devoid of CDK1/2 activities, PML protein was up-regulated because of a resistance to KLHL20-mediated degradation (Figures S3C and S3D). We next determined whether PML is a substrate of CDK1/2. Purified Flag-PML-I was efficiently phosphorylated by CDK2-cyclin E or CDK1-cyclin B complex in vitro (Figure 3C). Further analysis using various PML mutants demonstrated S518 as the prime residue targeted by CDK2-cyclin E and CDK1-cylcin B (Figure 3C; Figures S3E and S3F). However, CDK6-cyclin D only modestly phosphorylated PML in vitro (Figure 3C), which may account for its inability to promote KLHL20-mediated PML degradation in vivo. To assess PML S518 phosphorylation in vivo, we generated an antibody that recognizes S518-phosphorylated PML. This antibody reacted with WT PML-I and PML-I S527A, but not with PML-I S518A (Figure S3G). With this antibody, we showed that roscovitine compromised S518 phosphorylation of endogenous PML in multiple cell lines (Figure S3H). Furthermore, DN mutant of CDK1 or CDK2 blocked, whereas overexpression of CDK1-cyclin B

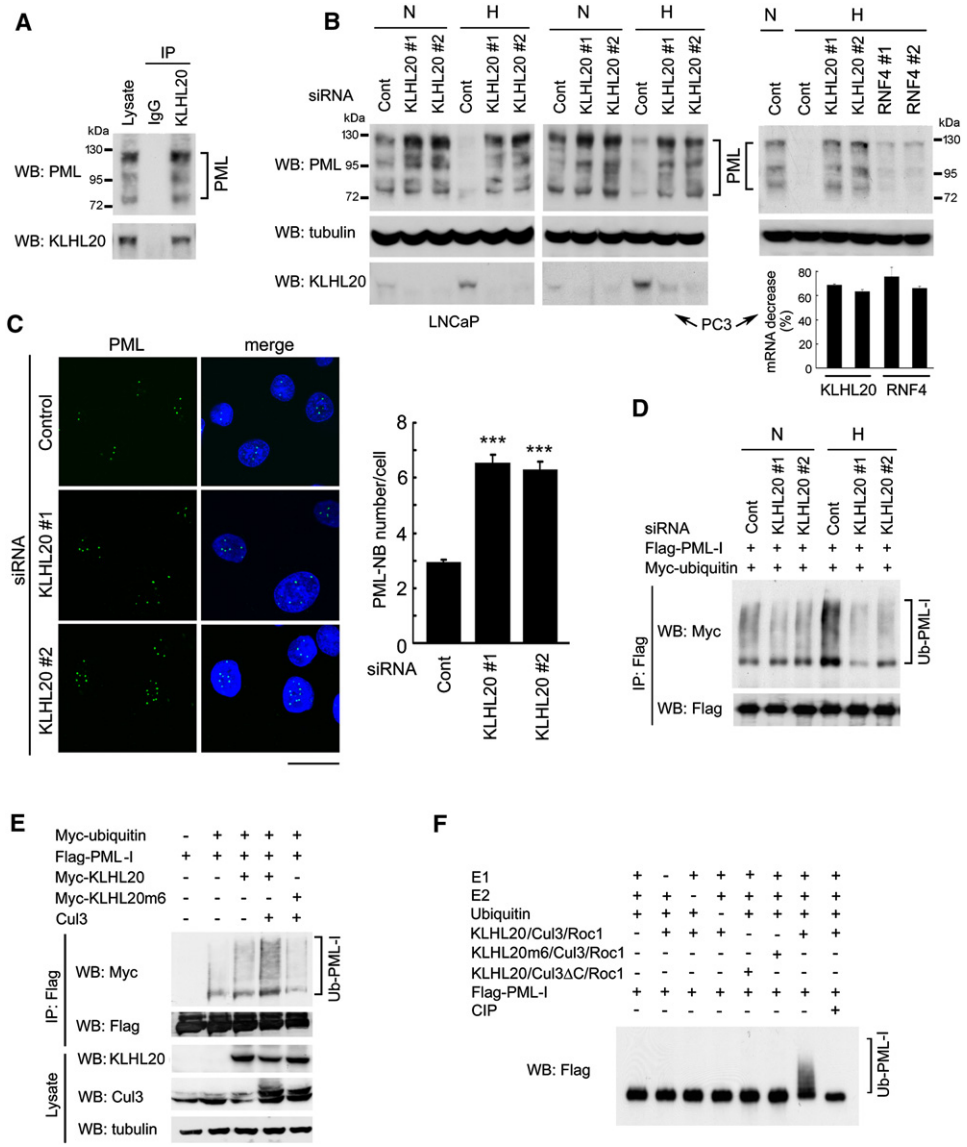

Figure 2. KLHL20 Mediates PML Ubiquitination and Destruction in Hypoxic and Normoxic Cells

(A) KLHL20 interacts with PML in PC3 cells treated with hypoxia and MG132 for 24 hr.

(B) Western blot analysis of PML level in LNCaP or PC3 cells stably expressing indicated siRNA and cultured under normoxia or hypoxia for 24 hr. The knockdown efficiency of individual siRNA in each cell line was determined by RT/qPCR and is presented as percentage of decrease in mRNA level (bottom).

(C) KLHL20 down-regulates PML-NBs in hypoxic cells. Cells as in (B) were cultured in hypoxia for 24 hr, stained with PML antibody and DAPI, and examined by confocal microscopy. The representative immunofluorescent image (left) and the average PML-NB numbers per cell calculated from 60 cells in each population (right) are presented. Scale bar, 20 μm.

(D and E) KLHL20 promotes PML ubiquitination in vivo. LNCaP cells stably expressing various siRNAs (D) or HeLa cells transfected with indicated constructs (E) were examined for PML ubiquitination as in Figure 1D.

(F) In vitro ubiquitination of PML by KLHL20-Cul3-Roc1 complex. Flag-PML-I purified from baculovirus and pretreated with or without CIP was subject to in vitro ubiquitination reaction in the presence of E1, E2, E3 complex and/or ubiquitin (see Experimental Procedures), and examined by western blot with anti-Flag antibody. Results in (B) and (C) are presented as mean ± SD (***$p < 0.0005$, $n = 3$).

See also Figure S2.

or CDK2-cyclin E enhanced S518 phosphorylation in vivo (Figure 3D). These results indicate a direct and physiological role of CDK1/2 in phosphorylating PML at S518, which in turn promotes PML ubiquitination by the Cul3-KLHL20 ligase.

The identification of an essential role of CDK1/2 in KLHL20-mediated PML ubiquitination raised a concern as to whether the same kinases mediate PML ubiquitination in hypoxia conditions, given that prolonged hypoxia treatment of certain cells results in cell cycle arrest. We thus evaluated the influence of hypoxia on CDK1/2 activities. Of note, PML down-regulation was observed as early as 8 hr of hypoxia treatment, and only a trace amount of PML was detected at 24 hr of treatment

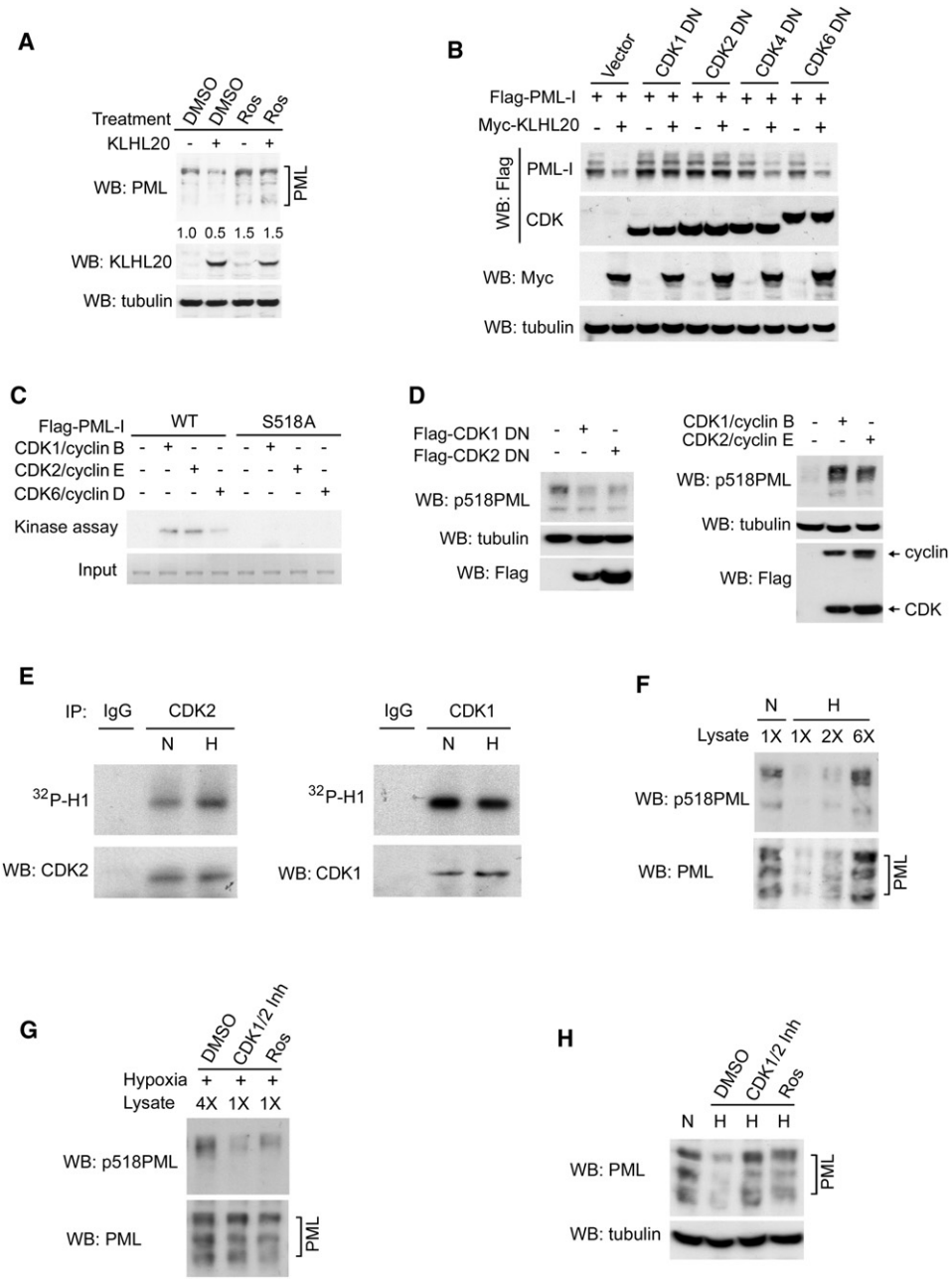

Figure 3. CDK1 and CDK2 Phosphorylate PML in Both Normoxia and Hypoxia to Promote KLHL20-Induced PML Destruction

(A) Western blot analysis of endogenous PML in 293T cells transfected with KLHL20 and/or treated with roscovitine. The relative levels of PML are indicated.

(B) DN mutant of CDK1 or CDK2 blocks KLHL20-induced PML-I degradation in 293T cells.

(C) Purified PML-I and its mutant were phosphorylated by indicated CDK-cyclin complexes in vitro and were analyzed by autoradiography (top). Equal inputs of various substrates were assessed by Coomassie blue staining (bottom).

(D) Western blot analysis of PML S518 phosphorylation in 293T cells overexpressing indicated CDK DN mutant (left) or CDK-cyclin complex (right).

(E) Kinase activities of CDK1 and CDK2 immunoprecipitated from PC3 cells cultured in normoxia or hypoxia for 24 hr were assayed by in vitro phosphorylation of histone H1. The input of CDK1/2 is shown on the bottom.

(F) Western blot analysis of PML S518 phosphorylation in PC3 cells cultured as in (E).

(G and H) Western blot analysis of S518-phosphorylated PML (G) and total PML (H) in PC3 cells cultured as in (E) and treated with indicated inhibitors for 24 hr. To ensure an accurate comparison, different amounts of lysate from hypoxic cells were loaded in (F) and (G).

See also Figure S3.

(see Figure 1A). However, the activities of CDK1 and CDK2 (Figure 3E) as well as the PML S518 phosphorylation level (Figure 3F) were not decreased by 24 hr treatment of hypoxia. Furthermore, no significant difference in the cell cycle profiles of multiple cancer cell lines was observed at this time point, even though an enrichment of G1 population was detected 1 day later (Figure S3I). These observations suggest the capability of CDK1/2 in phosphorylating PML during the period of hypoxia when KLHL20 is highly induced to promote PML ubiquitination. In keeping with this notion, roscovitine or a CDK1/2-specific inhibitor diminished PML S518 phosphorylation (Figure 3G) and degradation (Figure 3H) in hypoxia. Thus, CDK1/2 is involved in PML destruction in both normoxia and hypoxia conditions.

In contrast to the normoxia and hypoxia conditions, the activities of CDK1/2 and PML S518 phosphorylation were severely compromised in an ischemia-mimetic cell culture system (Figures S3J and S3K). In line with the requirement of CDK1/2 in KLHL20-mediated PML degradation, PML protein was accumulated under this condition (Figure S3K, bottom), which is consistent with a previous study performed in a muscle ischemia model (Bernardi et al., 2006). These findings suggest a biphasic regulation of PML stability with the drop of oxygen concentrations.

S518 Phosphorylation and Pin1-Mediated Prolylisomerization Promote the Recruitment of PML to KLHL20

To further understand the influence of CDK1/2-mediated phosphorylation on PML ubiquitination by Cul3-KLHL20, we used the phosphorylation-defective mutant PML-I S518A. Unlike the wild-type protein, this mutant could no longer interact with KLHL20 both in vivo (Figure 4A) and in vitro (Figure S4A) and was defective in KLHL20-induced ubiquitination (Figure 4B) and degradation (Figure S4B). More importantly, the S518A mutant was turned over more slowly than wild-type protein in hypoxia, and this difference in turnover rate was abrogated by KLHL20 depletion (Figure 4C). These results support a notion that S518 phosphorylation facilitates the recruitment of PML to Cul3-KLHL20 for ubiquitination and, subsequently, degradation.

A previous study revealed that PML phosphorylated at four pS-P motifs, including the pS518-P519 motif, promotes its degradation mediated by Pin1 (Reineke et al., 2008). We found that S518 mutation blocked PML interaction with Pin1 both in vivo (Figure 4D) and in vitro (Figure S4C). In viewing of the prime role of pS518-P519 motif in Pin1 binding, we thought to test a model whereby Pin1-mediated isomerization on CDK-phosphorylated PML potentiates the recruitment of PML to Cul3-KLHL20 for ubiquitination. In keeping with this model, although CDK1-mediated phosphorylation enhanced PML ubiquitination by KLHL20-Cul3-Roc1 in vitro, incubation of CDK-phosphorylated PML with Pin1, but not its substrate binding–defective mutant Pin1 W34A, further augmented this ubiquitination (Figure S4D). Consistent with this in vitro finding, Pin1 silencing abolished PML-I interaction with KLHL20 (Figure S4E) and ubiquitination by KLHL20-Cul3 in vivo (Figure 4E). Consequently, KLHL20-induced down-regulations of PML-I (Figure S4F) and endogenous PML (Figure S4E, bottom) were blocked. Pin1 depletion also abrogated hypoxia-induced PML destruction (Figure 4F). Collectively, our study uncovers a PML degradation pathway, in which sequential modifications of PML by CDK1/2 and Pin1 at the S518-P519 motif facilitate the recruitment of PML to Cul3-KLHL20 for ubiquitination. Under hypoxia conditions, the drastic up-regulation of KLHL20 leads to a robust PML ubiquitination through this pathway, thereby greatly reducing PML abundance. Notably, the S518 and P519 residues are present in PML isoforms I to VI (Bernardi and Pandolfi, 2007) and are evolutionarily conserved (Figure S3L), thus highlighting the importance and prevalence of this pathway in regulating PML abundance.

KLHL20-Mediated PML Destruction Amplifies Tumor Hypoxia Responses

A previous report indicates that PML is itself a negative regulator of HIF-1α protein synthesis through a repression of mTOR activity (Bernardi et al., 2006). Accordingly, knockdown of PML in PC3 cells enhanced hypoxia-induced HIF-1α (Figure S5A). Thus, the HIF-1α-induced, KLHL20-mediated PML destruction pathway may function to derepress mTOR and HIF-1α, thereby participating in a double-negative feedback loop to amplify HIF-1α signaling. In line with this notion, depletion of KLHL20 in PC3 cells led to an enhanced decline of mTOR activity (monitored by the phosphorylation of mTOR downstream molecules S6 kinase and S6) and a decreased induction of HIF-1α in response to hypoxia treatment (Figure 5A). More importantly, depletion of PML in the KLHL20-knockdown cells completely rescued mTOR activity and HIF-1α induction (Figure 5A), indicating the involvement of PML in KLHL20 siRNA-induced mTOR and HIF-1α down-regulation. The KLHL20-PML pathway also led to an increased HIF-2α induction under more stringent hypoxia conditions (Figure S5B). Conceivably, KLHL20-depleted cells exhibited a lower induction of HIF targets *VEGF* (Figure S5C) and *GLUT1* (Figure 5B) than did control siRNA-expressing cells, and depletion of both KLHL20 and PML reversed these effects. Thus, the KLHL20-PML pathway is critical for hypoxic cells to achieve a full induction of HIF signaling.

Next, we tested whether the influence of KLHL20-PML pathway on HIF induction could potentiate tumor hypoxia responses. Hypoxia treatment of control siRNA-expressing PC3 cells resulted in a decrease of apoptosis induced by doxorubicin, and this effect was enhanced by PML knockdown (Figure 5C). Importantly, the chemoresistance effect of hypoxia was abrogated by KLHL20 silencing and was rescued by KLHL20 and PML double knockdown (Figure 5D). Similar to many other tumor cells, hypoxia treatment of control siRNA-expressing PC3 cells induced epithelial-mesenchymal transition (EMT), as evidenced by morphological changes, down-regulation of E-cadherin, and up-regulation of N-cadherin and vimentin (Figure 5E), and promoted migration (Figure 5F, bottom). Remarkably, these effects were all attenuated by KLHL20 silencing and rescued by double knockdown of KLHL20 and PML. PML knockdown alone moderately enhanced hypoxia-induced cell migration (Figure 5F, top), in line with the elevation of HIF-1α under such conditions. Collectively, our findings indicate that the KLHL20-PML pathway is part of a feedback control mechanism to amplify HIF-1-mediated tumor hypoxia responses.

If KLHL20-PML pathway indeed participates in the HIF-1 feedback regulation, overexpression of a nondegradable mutant PML S518A should disrupt this feedback loop. We thus stably expressed this mutant in PC3 cells. For comparison, wild-type

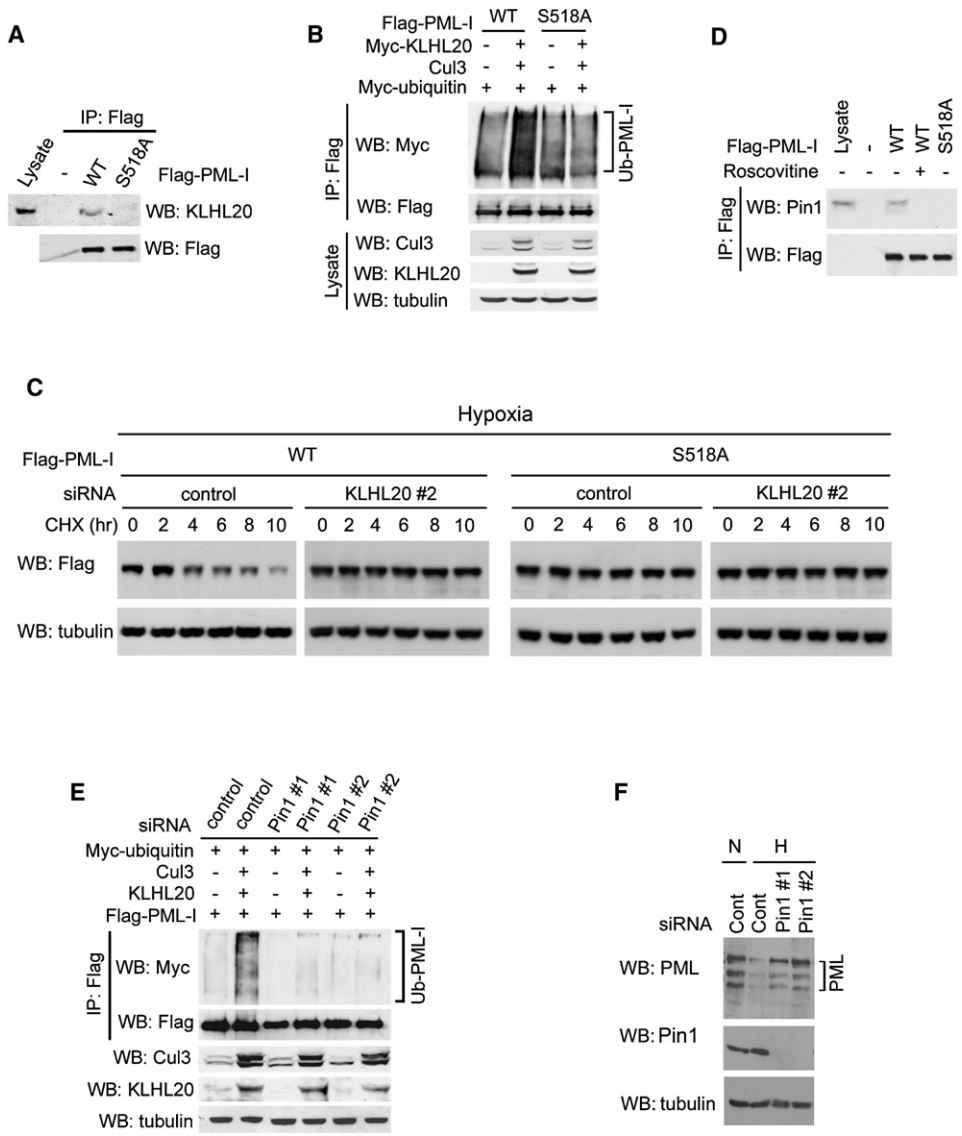

Figure 4. S518 Phosphorylation Mediates Pin1-Dependent Prolylisomerization to Promote PML Targeting to KLHL20

(A) PML-I, but not PML-I S518A, coimmunoprecipitated endogenous KLHL20 from 293T transfectants.

(B) S518 mutation impairs KLHL20-dependent PML ubiquitination. 293T cells transfected with indicated constructs were assayed for PML-I ubiquitination.

(C) Western blot analysis of the turnover rate of PML-I and its mutant in hypoxic LNCaP cells expressing indicated siRNA and treated with CHX.

(D) 293T cells expressing Flag-PML-I or its mutant were treated with or without roscovitine, and then were analyzed for PML/Pin1 interaction by immunoprecipitation.

(E) Pin1 promotes KLHL20-dependent PML ubiquitination. 293T cells expressing control or Pin1 siRNA were transfected with indicated constructs and then were assayed for PML-I ubiquitination.

(F) Pin1 mediates hypoxia-induced PML destruction. PC3 cells stably expressing indicated siRNAs were cultured in normoxia or hypoxia and were analyzed by western blot.

See also Figure S4.

PML was also introduced. As expected, PML S518A was accumulated to a higher level than wild-type protein, despite their comparable mRNA levels (Figure 6A). Remarkably, PML S518A overexpression abrogated HIF-1α induction and hypoxia-induced *GLUT1* expression, chemoresistance, and migration (Figures 6B–6E). These hypoxia responses, however, were still observed in cells expressing wild-type PML, albeit reaching to lower extents in comparison with the parental PC3 cells. These findings further support the impact KLHL20-mediated PML degradation on amplifying HIF-1 signaling.

KLHL20-Mediated PML Destruction Elicits Tumor-Promoting Functions Under Normoxia Conditions

Because KLHL20 potentiates PML degradation not only in hypoxic cells but also in normoxic cells, we surmised that the KLHL20-PML pathway may contribute to certain tumor-promoting

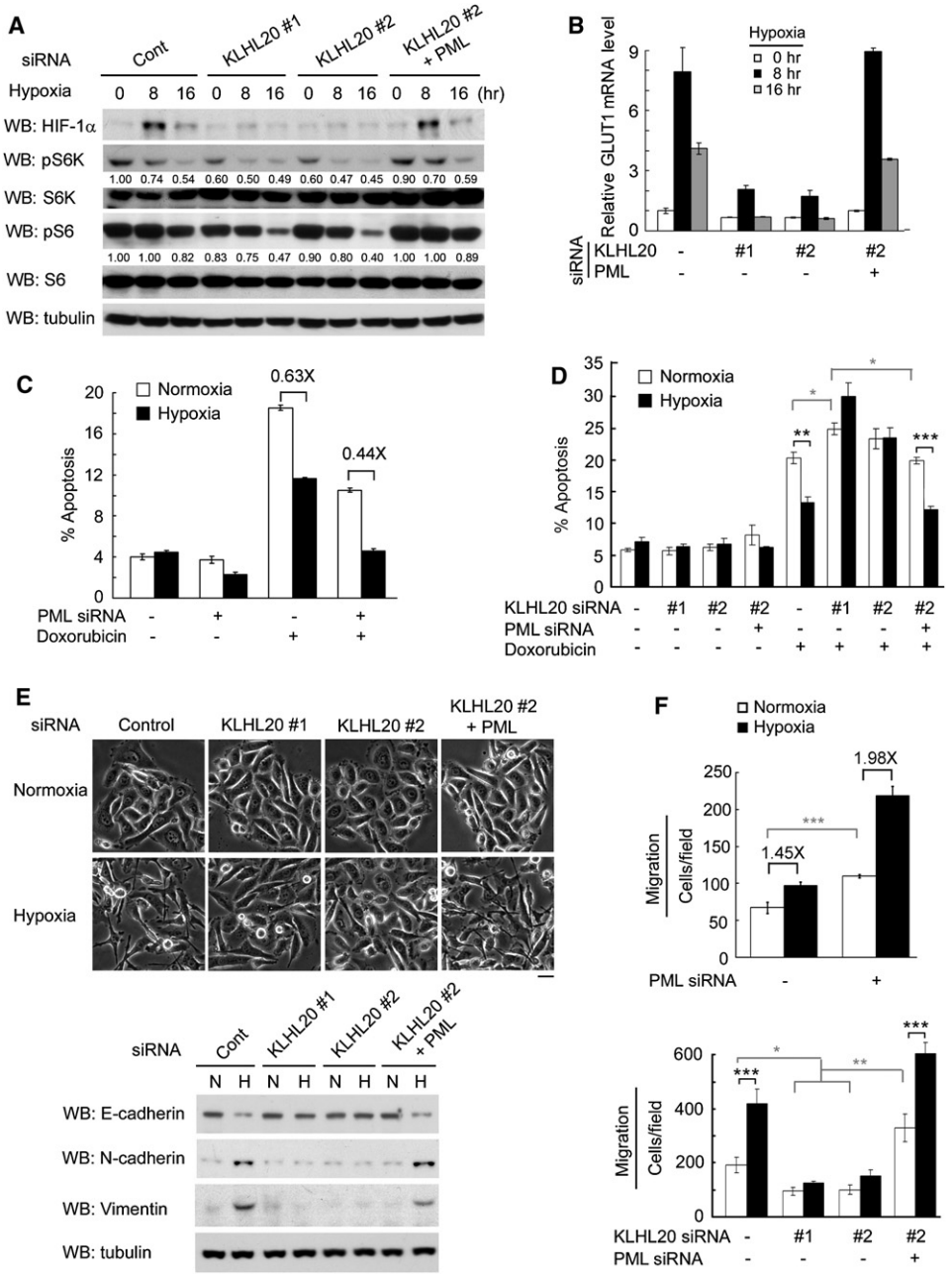

Figure 5. KLHL20-Mediated PML Destruction Amplifies HIF-1 Signaling

(A and B) Western blot analysis of phospho-S6 kinase (pS6K), S6 kinase, phospho-S6 (pS6), S6, and HIF-1α (A), and RT-qPCR analysis of *GLUT1* (B) in PC3 cells stably expressing indicated siRNAs and treated with hypoxia for various time points. The relative amounts of pS6K and pS6, normalized to their total levels, are indicated. The expression levels of KLHL20 and PML in these stable lines are shown in Figure S6A (lanes 1, 5, 6, and 7).

(C and D) Apoptosis assays of PC3 cells expressing indicated siRNAs and treated with or without doxorubicin in hypoxia or normoxia.

(E) EMT assays for cells as in (A) cultured in normoxia or hypoxia for 24 hr. The cell morphology was visualized by phase-contrast microscopy (top), whereas the expression of E-cadherin, N-cadherin, and vimentin was determined by western blot (bottom). Scale bar, 20 μm.

(F) PC3 cells expressing indicated siRNAs were assayed for migration under normoxia or hypoxia for 12 hr (top) or 16 hr (bottom). Data in (B), (C), (D), and (F) are presented as mean ± SD (*$p < 0.05$, **$p < 0.005$, ***$p < 0.0005$, $n = 3$).

See also Figure S5.

functions in normoxia. Indeed, depletion of KLHL20 in PC3 cells led to a reduction in forming soft-agar colonies, and this effect was rescued by double depletion of KLHL20 and PML (Figure S5D). KLHL20 silencing in normoxia also decreased cell migration (Figure 5F, bottom, gray brackets) and modestly promoted doxorubicin-induced apoptosis (Figure 5D, gray brackets), and all these effects were rescued by combined depletion of KLHL20 and PML. Consistent with a previous report (Reineke et al.,

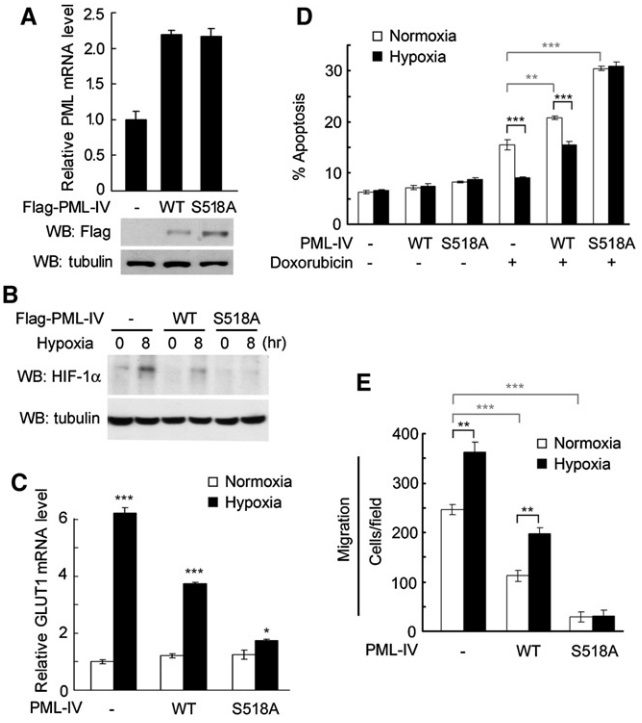

Figure 6. PML S518A Blocks HIF-1α Induction and Tumor Hypoxia Responses

(A) PC3 cells transduced with indicated lentivirus were analyzed for total *PML* mRNA expression and PML-IV protein expression by RT/PCR and western blot, respectively.

(B and C) Cells as in (A) were exposed to hypoxia for 0 or 8 hr and then were assayed for HIF-1α expression by western blot and for *GLUT1* expression by RT-PCR.

(D) Apoptosis assay of cells as in (A) treated with or without doxorubicin under normoxia or hypoxia.

(E) Cells as in (A) were assayed for migration in normoxia or hypoxia for 16 hr. Data in (A), (C), (D), and (E) are presented as mean ± SD (*$p < 0.05$, **$p < 0.005$, ***$p < 0.0005$, n = 3).

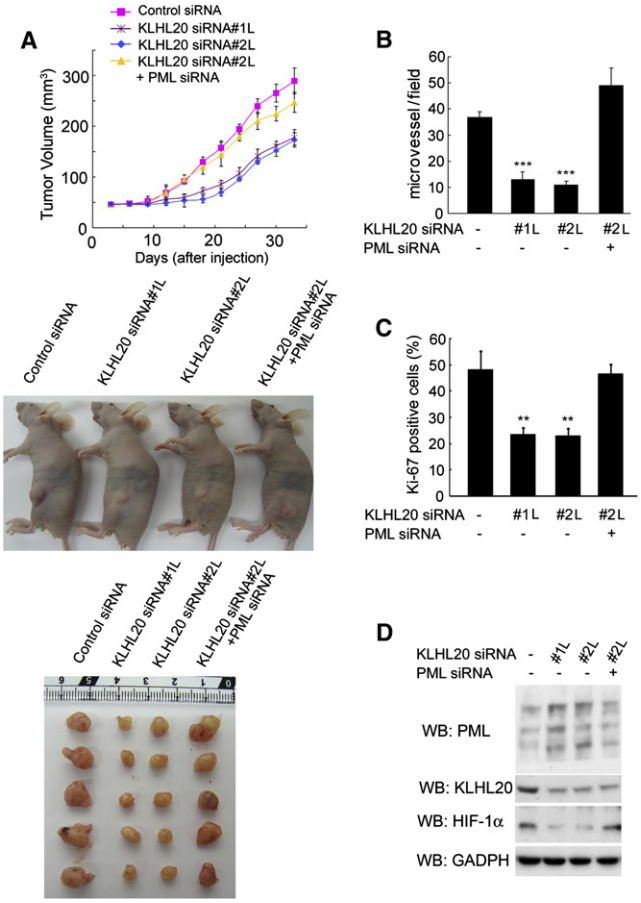

Figure 7. KLHL20-Mediated PML Destruction Promotes Tumor Angiogenesis and Growth

(A) Tumor growth of PC3 cells expressing indicated siRNA in a xenograft model.

(B and C) Quantitative data of CD31 (B) and Ki-67 (C) staining of comparable-sized tumors derived from indicated cells. Data are presented as mean ± SD (**$p < 0.005$, ***$p < 0.0005$, n = 3).

(D) Western blot analysis of the expression of PML, KLHL20, and HIF-1α in tumors derived from indicated cells.

See also Figure S6.

2010), PML depletion alone promoted migration in normoxia (Figure 5F, top, gray bracket). Conversely, overexpression of KLHL20-resistant PML S518A markedly potentiated apoptosis and inhibited migration in normoxia, whereas wild-type PML elicited weaker effects (Figures 6D and 6E, gray brackets). These findings support the contribution of KLHL20-PML pathway to tumor promotion in normoxia, even though the effect is less prominent than that observed in hypoxia.

KLHL20-Mediated PML Destruction Promotes Tumor Angiogenesis and Growth In Vivo

Next, we evaluated the influence of KLHL20-PML pathway on tumor growth and angiogenesis using xenograft models. To specifically assess angiogenesis, we generated tumor cell lines with comparable proliferation and transformation potencies. This was achieved by infecting PC3 cells with a low titer of lentivirus carrying KLHL20 siRNA. The transduced cells (KLHL20 siRNA #1L and KLHL20 siRNA #2L) as well as the KLHL20/PML double-depleted cells displayed lower KLHL20 knockdown efficiencies than aforementioned PC3 derivatives (Figure S6A). We confirmed that this new set of cell lines exhibited similar rate of proliferation in vitro and similar efficacy to form colonies in soft agar (Figures S6B and S6C). However, when they were injected into nude mice, their potency to form tumor was significantly different (Figure 7A). Tumors derived from KLHL20-depleted cells were smaller than those from parental PC3 cells or from cells depleted both KLHL20 and PML. Immunohistochemistry (IHC) analyses using tumors with a comparable size (~180 mm^3) revealed that tumors derived from KLHL20-depleted cells had significant lower microvessel density and proliferation rate than those from cells expressing control siRNA or both PML and KLHL20 siRNAs, as determined by CD31 and Ki67 staining, respectively (Figures 7B and 7C; Figures S6D and S6E). The KLHL20-depleted tumors also exhibited higher PML and lower HIF-1α levels than similar-sized tumors from other two groups (Figure 7D; Figure S6F). Consistent with a previous report (Bernardi et al., 2006), PML depletion alone did not significantly altered soft-agar colony formation of PC3 cells,

but enhanced tumor growth, angiogenesis, and HIF-1α induction in xenograft model (Figures S6G–S6I). Thus, the KLHL20-induced PML destruction pathway promotes tumor angiogenesis and tumor growth in vivo, and these functions are mediated at least in part through the elevation of HIF-1 signaling.

HIF-1α/KLHL20/Pin1/PML Pathway Is Manifested in Human Prostate Cancer and Is Up-Regulated in High-Grade Tumors

To validate the clinical relevance of KLHL20-mediated PML destruction pathway to human cancer and its contribution to PML down-regulation in tumors, we analyzed the expression profiles of HIF-1α, Pin1, KLHL20, and PML in consecutive slides from 79 human prostate cancer patients and 17 benign prostate hyperplasia (BPH) cases. Remarkably, IHC analysis revealed drastic differences in the expression levels of these four proteins between tumor and BPH, and representative images are shown in Figures S7A and S7B. Compared to BPH, tumor specimens exhibited significant up-regulations of HIF-1α, KLHL20, and Pin1 and down-regulation of PML (Figure 8A). In addition, we found that PML expression was inversely correlated with Pin1, KLHL20, and HIF-1α expression, whereas a positive correlation was observed between the expression of HIF-1α and KLHL20 (Figure 8B). These findings support the existence of HIF-1α/KLHL20/Pin1/PML pathway in human prostate cancer. More importantly, the percentage of patients displaying the signature of high HIF-1α, high KLHL20, high Pin1, and low PML expression pattern, which suggests a hyperactive feature of the PML destruction pathway, was progressively increased with the increase of tumor grade, and a significant difference was observed between each of the three groups: prostatic intraepithelial neoplasia (PIN), Gleason score 6/7, and Gleason score $\geq$ 8 (Figure 8C). These findings suggest a relevance of the HIF-1α/Pin1/KLHL20/PML signaling axis to tumor progression.

DISCUSSION

Our study reveals a central role of the Cul3 substrate adaptor KLHL20 in the regulation of hypoxia responses and tumor progression (Figure 8D, top). KLHL20 is transcriptionally up-regulated by HIF-1 and mediates hypoxia-induced PML polyubiquitination. However, efficient recruitment of PML to KLHL20 requires two consecutive posttranslational modifications at PML S518-P519, phosphorylation by CDK1/2, and prolyl *cis/trans* isomerization by Pin1. Importantly, this HIF-1-induced, KLHL20-mediated PML destruction, together with the PML-induced, mTOR-mediated HIF-1α repression (Bernardi et al., 2006), constitutes a double-negative feedback loop to amplify HIF-1 signaling. The pathophysiological significance of this HIF-1α feedback control is evidenced by the finding that KLHL20 silencing compromises multiple tumor hypoxia responses, which are all rescued by double depletion of KLHL20 and PML. Furthermore, ectopic expression of KLHL20-resistant PML S518A similarly abrogates tumor hypoxia responses. Besides amplifying HIF-1 signaling, KLHL20 also potentiates PML degradation. Because these two events elicit partially overlapping biological functions, such as promoting migration and survival, they could act in synergism to contribute to tumor progression in hypoxia. The clinical relevance of our findings is supported by the observations that PML down-regulation correlates with HIF-1α, Pin1, and KLHL20 up-regulation in human prostate cancer and that hyperactivation of this pathway correlates with high-grade tumors. Given that overexpression of HIF-1α is widespread in human cancers through hypoxic or non-hypoxic mechanism (Henze and Acker, 2010), the impact of HIF-1-KLHL20-PML pathway may extend beyond the prostate cancer, and thus our study may provide molecular insights into PML down-regulation in diverse cancer types (Gurrieri et al., 2004).

It is worth noting that HIF-1α is induced transiently under hypoxia conditions, and several negative feedback regulatory mechanisms are responsible for its down-regulation during prolonged hypoxia (Henze and Acker, 2010). This raises the question why the positive feedback regulation of HIF-1α, as described in this study, evolved and how this regulation could be beneficial for tumor progression. Because tumor cells are often subject to microenvironments with fluctuating oxygen concentrations (Henze and Acker, 2010), the positive feedback regulation of HIF-1α allows a rapid and robust induction of hypoxia responses, which could be exploited by tumor to ensure a timely adjustment during acute hypoxia conditions, thereby maintaining cell homeostasis and survival. However, in response to chronic hypoxia, the KLHL20-mediated HIF-1α feedback control may be dampened because of the decrease of CDK1/2 activities, as deduced by an enrichment of G1-arrested cells (Figure S3I). This adjustment, together with the activation of various negative feedback mechanisms, would lead to an ultimate decline of HIF-1α level, thus allowing tumor cells to reset their threshold for HIF-1α induction in response to the next run of hypoxia stimulation.

Although this study reveals the participation of KLHL20-mediated PML degradation in HIF-1 feedback regulation, we do not exclude the involvement of other NB-residing proteins in KLHL20-regulated HIF-1 signaling. Furthermore, it is possible that a proteasome-independent mechanism also contributes to PML down-regulation during hypoxia. In addition, despite the down-regulation of PML in tumor cells, tumor-associated endothelial cells and infiltrating lymphocytes often exhibit large number of PML-NBs (Gurrieri et al., 2004), implying the existence of cell type–specific regulation of PML. Alternatively, this difference may occur at the level of PML-NB assembly, because regulation of PML protein and PML-NB assembly can be uncoupled in certain circumstances, including hypoxia conditions.

Previous studies indicated that phosphorylation at S565 by CK2 (Scaglioni et al., 2006) and sumoylation at K160 (Lallemand-Breitenbach et al., 2001) promote PML ubiquitination. Although the ubiquitin ligase RNF4 acts selectively on K160-sumoylated PML (Lallemand-Breitenbach et al., 2008), KLHL20-based E3 ligase can efficiently catalyze unsumoylated PML. Furthermore, S565 phosphorylation is likely dispensable for targeting PML to KLHL20, because CK2 inactivation does not affect PML degradation by KLHL20 (Figure S3A). Nevertheless, we show that ubiquitination catalyzed by KLHL20-associated E3 ligase requires phosphorylation and prolylisomerization on the S518-P519 motif of PML. Because this motif is evolutionally conserved and present in most PML isoforms, the KLHL20-PML pathway likely represents a general mechanism for modulating PML stability under hypoxia conditions. Notably, this motif

A

	Expression	Benign (n=17)	Tumor (n=79)	p value*
HIF-1α	High	5 (29.4%)	47 (59.5%)	
	Low	12 (70.6%)	32 (40.5%)	p=0.032
KLHL20	High	4 (23.5%)	51 (64.6%)	
	Low	13 (76.5%)	28 (35.4%)	p=0.0027
Pin1	High	4 (23.5%)	59 (74.7%)	
	Low	13 (76.5%)	20 (25.3%)	p=0.0001
PML	High	13 (76.5%)	24 (30.4%)	
	Low	4 (23.5%)	55 (69.6%)	p=0.0007

* Fisher's exact test

B

	Expression	KLHL20 High	KLHL20 Low	p value*
HIF-1α	High	40	12	
	Low	15	29	p=0.00003

	Expression	HIF-1α High	HIF-1α Low	p value*
PML	High	15	22	
	Low	37	22	p=0.038

	Expression	KLHL20 High	KLHL20 Low	p value*
PML	High	12	25	
	Low	43	16	p=0.0001

	Expression	Pin1 High	Pin1 Low	p value*
PML	High	18	19	
	Low	45	14	p=0.008

* Fisher's exact test

C

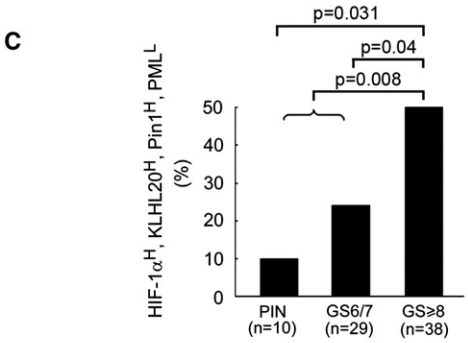

D

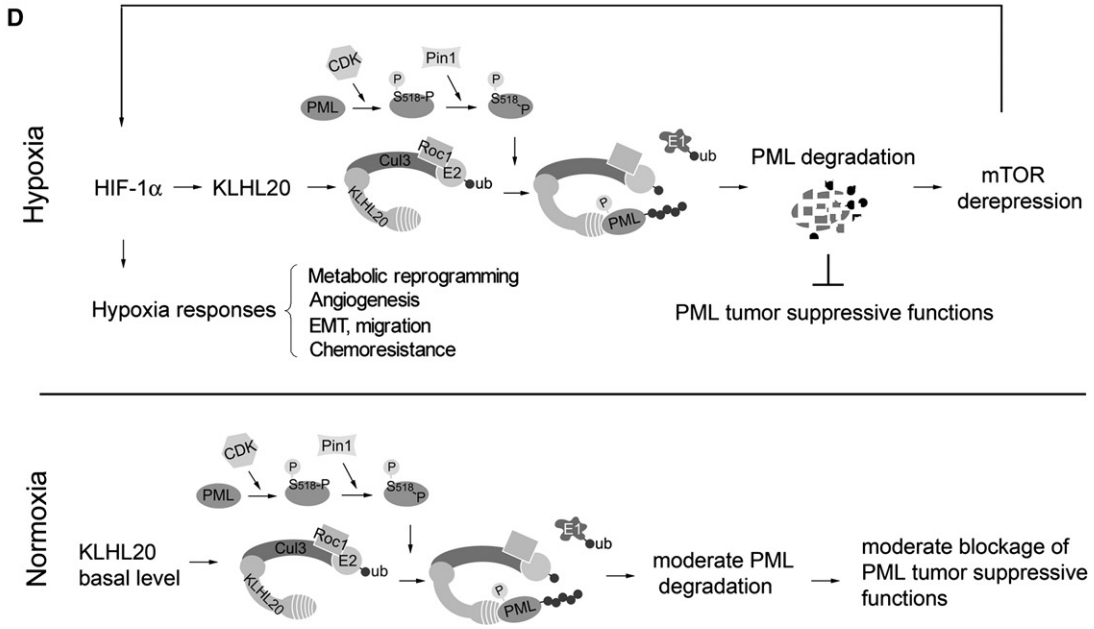

Figure 8. The HIF-1α/KLHL20/Pin1/PML Pathway Is Manifested in Human Prostate Cancer and Associated with High-Grade Tumor

(A) Summary of the HIF-1α, KLHL20, Pin1, and PML expression profiles.

(B) Positive correlation of KLHL20 and HIF-1α expression and inverse correlations of HIF-1α and PML expression, KLHL20 and PML expression, as well as Pin1 and PML expression in all 96 prostate specimens.

(C) Percentage of patients displaying the signature expression pattern of high HIF-1α, high KLHL20, high Pin1, and low PML in PIN, Gleason score (GS) 6 or 7, and GS $\geq$ 8. Total case number in each group is indicated on the bottom and patients without grade information were excluded. Fisher's exact test was used for comparison between groups.

(D) Model for KLHL20-mediated PML degradation in tumor development and progression under hypoxia and normoxia conditions.

See also Figure S7.

is also present in the oncogenic PML-RARα protein. Recent studies indicated a role of hypoxia and hypoxia-mimetic agent in stimulating the differentiation of acute myeloid leukemic cells (Huang et al., 2003; Liu et al., 2006), so it would be important to determine whether this effect is mediated by the degradation of PML-RARα through a KLHL20-dependent mechanism.

Although the KLHL20-dependent mechanism is responsible for hypoxia-induced PML destruction, we demonstrate that the same pathway also acts on normoxic cells to confer tumor-promoting functions, such as transformation, migration, and survival, albeit with a lower efficacy (Figure 8D, bottom). The requirement of CDK1/2 activities for targeting PML to KLHL20 in normoxia suggests the existence of a cell cycle–dependent regulation of PML. Accordingly, PML protein level is highest in G1, drops progressively in S and G2 (Dellaire et al., 2006), and is elevated in G1-arrested cells (Figures S3C and S3D). Future study will determine the impact of KLHL20-mediated PML degradation on cell cycle progression.

In summary, our study identifies a pathway by which KLHL20-mediated PML destruction controls the robust induction of HIF-1α. Although HIF-1α induction and PML destruction could act coordinately and/or synergistically to promote tumor progression in hypoxia, the latter also contributes to tumor promotion in normoxia. Thus, this pathway not only provides molecular insights into aberrant PML down-regulation in human cancers but also plays a crucial and versatile role in tumor development. Blockage of this pathway may potentially be a therapeutic strategy for treating human prostate cancer and other types of cancers.

EXPERIMENTAL PROCEDURES

Plasmids

Plasmids encoding Flag-KLHL20, Myc-KLHL20, Myc-KLHL20m6, Myc-ubiquitin, Myc-hCul3, Myc-Roc1, and Cul3△C were described previously (Lee et al., 2010). To clone *KLHL20* promoter, a DNA fragment corresponding to nucleotides −397 to +1102 of the *KLHL20* gene (numbered relative to the transcription initiation site) was amplified from the genomic DNA of 293 cells and inserted into the pGL3-Basic vector. Construct for HA-PML-IV was described elsewhere (Lin et al., 2006), whereas Flag-PML-I was a gift from Ming-Zong Lai. Constructs expressing Pin1 and its mutants were described elsewhere (Lu et al., 1996; Zhou et al., 2000). The full-length cDNAs for CDK1, CDK2, CDK4, and CDK6 were amplified by RT-PCR using total RNAs from HeLa cells and then subcloned to pRK5F or pRK5M vector. PML mutants, CDK mutants (CDK1 D146N, CDK2 D145N, CDK4 D158N, and CDK6 D163N), and *KLHL20* promoter mutants were generated by site-directed mutagenesis. HIF-1α and HIF-1α(△ODD) were provided by Kou-Juey Wu. To generate lentiviral and baculoviral expression constructs, PML-IV and PML-I were amplified by PCR and cloned to pLenti6-GW-V5 and pVL1392 vectors, respectively.

In Vitro and In Vivo Ubiquitination

For in vitro ubiquitination, 300 ng of baculovirally purified Flag-PML-I was treated with 0.75 unit of CIP or phosphorylated by CDK1-cyclin B (see Supplemental Experimental Procedures), and/or incubated with 200 ng of GST-Pin1 (or its mutant) at 4°C for 1 hr. Roc1-Cul3-KLHL20 complex was purified using Glutathione-Sepharose beads from lysates of 293T cells transfected with GST-Cul3, Myc-KLHL20, and Myc-Roc1. The purified complex bound on beads was incubated at 37°C for 4 hr in 20 μl reaction mixture containing 50 mM Tris (pH 7.5), 1 μM ubiquitin aldehyde, 20 μM MG132, 5 mM $MgCl_2$, 2 mM ATP, 2 mM NaF, 1 mM DTT, 10 μg ubiquitin, 10 mM creatine phosphate, 500 ng creatine kinase, 40 ng yeast E1 enzyme, 500 ng E2 enzyme (UbcH5a), and 300 ng PML-I.

For analyzing in vivo ubiquitination of PML, cells were transfected with various constructs together with myc-ubiquitin and Flag-PML-I or Flag-PML-IV and treated with MG132 for 16 hr. Cells were lysed by RIPA lysis buffer, and lysates were used for immunoprecipitation with anti-Flag antibody followed by western blot with anti-myc antibody. Alternatively, cells were transfected with various constructs together with His-ubiquitin and Flag-PML-I and treated with MG132. Cells were lysed by buffer A (6 M guanidine-HCl, 0.1 M Na_2HPO_4/NaH_2PO_4 [pH 8.0], and 10 mM imidazole), and lysates were incubated with Ni-NTA agarose for 3 hr at 4°C. The beads were washed once with buffer A, twice with buffer A/TI (1 vol buffer A: 3 vol buffer TI [25 mM Tris-HCl, pH 6.8, and 20 mM imidazole]), and three times with buffer TI, and then analyzed by western blot. In all experiments, equal expression of myc-ubiquitin or His-ubiquitin was verified by western blot analysis.

Apoptosis assay

Cells were cultured under normoxia or hypoxia conditions for 24 hr and then treated with 2 μg/ml doxorubicin for 24 hr under normoxia or hypoxia. Apoptotic cells were assayed by Annexin V-APC kit (BD PharMingen) and analyzed by flow cytometry.

Cell Migration Assays

For Transwell migration assay, the underside of Transwell polycarbonate membrane (8-μm pore size; Millipore) was coated with 30 ng/ml collagen I. 6×10^4 cells resuspended in serum-free medium containing 1% BSA were plated onto the upper chamber, and the medium containing 1% BSA and 10% FCS was added to the lower chamber. Cells were incubated at 37°C under normoxia or hypoxia. At the end point of incubation, cells that had migrated onto the lower membrane surface were fixed by 4% formaldehyde, stained with DAPI, and counted.

Tissue Specimens and IHC Analysis

Human prostate specimens were obtained from National Taiwan University Hospital Tissue Bank. All samples were deidentified prior to analysis. Studies involving these tissues were approved by the Institutional Review Boards at College of Medicine, National Taiwan University and Academia Sinica. For IHC staining, paraffin sections of 5 μm thickness on coating slides were heat-denatured with 10 mM sodium citrate buffer (pH 6.0) for 15 min for antigen retrieval and then incubated with anti-HIF-1α antibody (Novus, 1:25 dilution), anti-KLHL20 antibody (1:400 dilution), anti-PML antibody (1:50 dilution), or anti-Pin1 antibody (1:100 dilution). All staining procedures were performed using autostaining system (Ventana Medical System, Inc., Arizona) with basic DAB detection kit according to the manufacturer's protocol. The counterstaining was performed with hematoxylin. The IHC staining was scored as negative/weak positive (score 0), moderate positive (score 1+), and strong positive (score 2+) according to percentage of cells staining positive and staining intensity, and only the nuclear signal of HIF-1α was considered. For HIF-1α, Pin1, and KLHL20 staining, samples that showed strong positive (score 2+) were defined as high expression. For PML staining, because 62.5% of the specimens exhibited score 0, samples with score 1+ or 2+ were considered as high expression. IHC analysis on xenograft tumors was described in Supplemental Experimental Procedures.

Soft-Agar Colony-Formation Assay and Xenotransplantation

For assaying colony formation in soft agar, 2×10^4 PC3 derivatives were resuspended in 0.3% top agar. Colony formed after 3 weeks were stained by crystal violet and counted. For assaying tumor growth in xenograft model, 7-week-old BALB/c nude mice housed in specific pathogen-free conditions were injected s.c. with 2.5×10^6 PC3 derivatives (n = 7 for each group) mixed with PBS and Matrigel (vol/vol, 1:1). All mouse experiments were conducted with approval from the Experimental Animal Committee, Academia Sinica.

SUPPLEMENTAL INFORMATION

Supplemental Information includes seven figures and Supplemental Experimental Procedures and can be found with this article online at doi:10.1016/j.ccr.2011.07.008.

ACKNOWLEDGMENTS

We thank Ming-Zong Lai, Matthias Peter, and Kou-Juey Wu for providing reagents; National RNAi Core Facility for shRNA constructs and analysis with Cellomics Arrayscan HT fluorescence microscope; Hsuan-Yu Chen for instruction on statistical analyses; Chin-Chun Hung for confocal analysis;

and Hsin-Jien Kung and Hui-Kuan Lin for critical reading of the manuscript. This work was supported by NSC Frontier Grant NSC99-2321-B-001-081 and Academia Sinica Investigator Award. W.C. Yuan, Y.R. Lee and R.H. Chen designed the experiments and wrote the manuscript. W. C. Yuan, Y. R. Lee, T. Y. Chen, Y. M. Lin, H. Y. Chen, H. C. Chung, C. T. Chiang, C. K. Lai, L. T. Lu, and C. H. Chen performed the experiments. S. F. Huang performed IHC experiments on human specimens and analyzed the data. C. H. Tsai and P. W. Hsiao performed IHC experiments on mouse specimens and analyzed the data. D. L. Gu and Y. S. Jou analyzed the microarray data sets. Y. S. Pu provided prostate specimens. K. P. Lu and H. M. Shih provided cell lines, reagents, and intellectual input for the study.

Received: December 14, 2010
Revised: May 13, 2011
Accepted: July 12, 2011
Published: August 15, 2011

REFERENCES

Bernardi, R., and Pandolfi, P.P. (2007). Structure, dynamics and functions of promyelocytic leukaemia nuclear bodies. Nat. Rev. Mol. Cell Biol. *8*, 1006–1016.

Bernardi, R., Guernah, I., Jin, D., Grisendi, S., Alimonti, A., Teruya-Feldstein, J., Cordon-Cardo, C., Simon, M.C., Rafii, S., and Pandolfi, P.P. (2006). PML inhibits HIF-1alpha translation and neoangiogenesis through repression of mTOR. Nature *442*, 779–785.

Brahimi-Horn, M.C., Chiche, J., and Pouysségur, J. (2007). Hypoxia and cancer. J. Mol. Med. *85*, 1301–1307.

Condemine, W., Takahashi, Y., Zhu, J., Puvion-Dutilleul, F., Guegan, S., Janin, A., and de Thé, H. (2006). Characterization of endogenous human promyelocytic leukemia isoforms. Cancer Res. *66*, 6192–6198.

de Thé, H., Chomienne, C., Lanotte, M., Degos, L., and Dejean, A. (1990). The t(15;17) translocation of acute promyelocytic leukaemia fuses the retinoic acid receptor alpha gene to a novel transcribed locus. Nature *347*, 558–561.

de Thé, H., Lavau, C., Marchio, A., Chomienne, C., Degos, L., and Dejean, A. (1991). The PML-RAR alpha fusion mRNA generated by the t(15;17) translocation in acute promyelocytic leukemia encodes a functionally altered RAR. Cell *66*, 675–684.

Dellaire, G., Ching, R.W., Dehghani, H., Ren, Y., and Bazett-Jones, D.P. (2006). The number of PML nuclear bodies increases in early S phase by a fission mechanism. J. Cell Sci. *119*, 1026–1033.

Fanelli, M., Fantozzi, A., De Luca, P., Caprodossi, S., Matsuzawa, S., Lazar, M.A., Pelicci, P.G., and Minucci, S. (2004). The coiled-coil domain is the structural determinant for mammalian homologues of *Drosophila* Sina-mediated degradation of promyelocytic leukemia protein and other tripartite motif proteins by the proteasome. J. Biol. Chem. *279*, 5374–5379.

Finger, E.C., and Giaccia, A.J. (2010). Hypoxia, inflammation, and the tumor microenvironment in metastatic disease. Cancer Metastasis Rev. *29*, 285–293.

Gurrieri, C., Capodieci, P., Bernardi, R., Scaglioni, P.P., Nafa, K., Rush, L.J., Verbel, D.A., Cordon-Cardo, C., and Pandolfi, P.P. (2004). Loss of the tumor suppressor PML in human cancers of multiple histologic origins. J. Natl. Cancer Inst. *96*, 269–279.

Henze, A.T., and Acker, T. (2010). Feedback regulators of hypoxia-inducible factors and their role in cancer biology. Cell Cycle *9*, 2749–2763.

Huang, Y., Du, K.M., Xue, Z.H., Yan, H., Li, D., Liu, W., Chen, Z., Zhao, Q., Tong, J.H., Zhu, Y.S., and Chen, G.Q. (2003). Cobalt chloride and low oxygen tension trigger differentiation of acute myeloid leukemic cells: possible mediation of hypoxia-inducible factor-1alpha. Leukemia *17*, 2065–2073.

Ishov, A.M., Sotnikov, A.G., Negorev, D., Vladimirova, O.V., Neff, N., Kamitani, T., Yeh, E.T., Strauss, J.F., 3rd, and Maul, G.G. (1999). PML is critical for ND10 formation and recruits the PML-interacting protein daxx to this nuclear structure when modified by SUMO-1. J. Cell Biol. *147*, 221–234.

Jeanne, M., Lallemand-Breitenbach, V., Ferhi, O., Koken, M., Le Bras, M., Duffort, S., Peres, L., Berthier, C., Soilihi, H., Raught, B., and de Thé, H. (2010). PML/RARA oxidation and arsenic binding initiate the antileukemia response of As_2O_3. Cancer Cell *18*, 88–98.

Lallemand-Breitenbach, V., Zhu, J., Puvion, F., Koken, M., Honoré, N., Doubeikovsky, A., Duprez, E., Pandolfi, P.P., Puvion, E., Freemont, P., and de Thé, H. (2001). Role of promyelocytic leukemia (PML) sumolation in nuclear body formation, 11S proteasome recruitment, and As_2O_3-induced PML or PML/retinoic acid receptor alpha degradation. J. Exp. Med. *193*, 1361–1371.

Lallemand-Breitenbach, V., Jeanne, M., Benhenda, S., Nasr, R., Lei, M., Peres, L., Zhou, J., Zhu, J., Raught, B., and de Thé, H. (2008). Arsenic degrades PML or PML-RARalpha through a SUMO-triggered RNF4/ubiquitin-mediated pathway. Nat. Cell Biol. *10*, 547–555.

Lee, Y.R., Yuan, W.C., Ho, H.C., Chen, C.H., Shih, H.M., and Chen, R.H. (2010). The Cullin 3 substrate adaptor KLHL20 mediates DAPK ubiquitination to control interferon responses. EMBO J. *29*, 1748–1761.

Lin, D.Y., Huang, Y.S., Jeng, J.C., Kuo, H.Y., Chang, C.C., Chao, T.T., Ho, C.C., Chen, Y.C., Lin, T.P., Fang, H.I., et al. (2006). Role of SUMO-interacting motif in Daxx SUMO modification, subnuclear localization, and repression of sumoylated transcription factors. Mol. Cell *24*, 341–354.

Liu, W., Guo, M., Xu, Y.B., Li, D., Zhou, Z.N., Wu, Y.L., Chen, Z., Kogan, S.C., and Chen, G.Q. (2006). Induction of tumor arrest and differentiation with prolonged survival by intermittent hypoxia in a mouse model of acute myeloid leukemia. Blood *107*, 698–707.

Louria-Hayon, I., Alsheich-Bartok, O., Levav-Cohen, Y., Silberman, I., Berger, M., Grossman, T., Matentzoglu, K., Jiang, Y.H., Muller, S., Scheffner, M., et al. (2009). E6AP promotes the degradation of the PML tumor suppressor. Cell Death Differ. *16*, 1156–1166.

Lu, K.P., Hanes, S.D., and Hunter, T. (1996). A human peptidyl-prolyl isomerase essential for regulation of mitosis. Nature *380*, 544–547.

Maxwell, P.H., Wiesener, M.S., Chang, G.W., Clifford, S.C., Vaux, E.C., Cockman, M.E., Wykoff, C.C., Pugh, C.W., Maher, E.R., and Ratcliffe, P.J. (1999). The tumour suppressor protein VHL targets hypoxia-inducible factors for oxygen-dependent proteolysis. Nature *399*, 271–275.

Melnick, A., and Licht, J.D. (1999). Deconstructing a disease: RARalpha, its fusion partners, and their roles in the pathogenesis of acute promyelocytic leukemia. Blood *93*, 3167–3215.

Nacak, T.G., Alajati, A., Leptien, K., Fulda, C., Weber, H., Miki, T., Czepluch, F.S., Waltenberger, J., Wieland, T., Augustin, H.G., and Kroll, J. (2007). The BTB-Kelch protein KLEIP controls endothelial migration and sprouting angiogenesis. Circ. Res. *100*, 1155–1163.

Pintard, L., Willems, A., and Peter, M. (2004). Cullin-based ubiquitin ligases: Cul3-BTB complexes join the family. EMBO J. *23*, 1681–1687.

Reineke, E.L., Lam, M., Liu, Q., Liu, Y., Stanya, K.J., Chang, K.S., Means, A.R., and Kao, H.Y. (2008). Degradation of the tumor suppressor PML by Pin1 contributes to the cancer phenotype of breast cancer MDA-MB-231 cells. Mol. Cell. Biol. *28*, 997–1006.

Reineke, E.L., Liu, Y., and Kao, H.Y. (2010). Promyelocytic leukemia protein controls cell migration in response to hydrogen peroxide and insulin-like growth factor-1. J. Biol. Chem. *285*, 9485–9492.

Salomoni, P., and Pandolfi, P.P. (2002). The role of PML in tumor suppression. Cell *108*, 165–170.

Salomoni, P., Ferguson, B.J., Wyllie, A.H., and Rich, T. (2008). New insights into the role of PML in tumour suppression. Cell Res. *18*, 622–640.

Scaglioni, P.P., Yung, T.M., Cai, L.F., Erdjument-Bromage, H., Kaufman, A.J., Singh, B., Teruya-Feldstein, J., Tempst, P., and Pandolfi, P.P. (2006). A CK2-dependent mechanism for degradation of the PML tumor suppressor. Cell *126*, 269–283.

Semenza, G.L. (2010). Defining the role of hypoxia-inducible factor 1 in cancer biology and therapeutics. Oncogene *29*, 625–634.

Tatham, M.H., Geoffroy, M.C., Shen, L., Plechanovova, A., Hattersley, N., Jaffray, E.G., Palvimo, J.J., and Hay, R.T. (2008). RNF4 is a poly-SUMO-specific E3 ubiquitin ligase required for arsenic-induced PML degradation. Nat. Cell Biol. *10*, 538–546.

Trotman, L.C., Alimonti, A., Scaglioni, P.P., Koutcher, J.A., Cordon-Cardo, C., and Pandolfi, P.P. (2006). Identification of a tumour suppressor network opposing nuclear Akt function. Nature *441*, 523–527.

Wang, G.L., Jiang, B.H., Rue, E.A., and Semenza, G.L. (1995). Hypoxia-inducible factor 1 is a basic-helix-loop-helix-PAS heterodimer regulated by cellular O2 tension. Proc. Natl. Acad. Sci. USA *92*, 5510–5514.

Wang, Z.G., Delva, L., Gaboli, M., Rivi, R., Giorgio, M., Cordon-Cardo, C., Grosveld, F., and Pandolfi, P.P. (1998). Role of PML in cell growth and the retinoic acid pathway. Science *279*, 1547–1551.

Zhou, X.Z., Kops, O., Werner, A., Lu, P.J., Shen, M., Stoller, G., Küllertz, G., Stark, M., Fischer, G., and Lu, K.P. (2000). Pin1-dependent prolyl isomerization regulates dephosphorylation of Cdc25C and tau proteins. Mol. Cell *6*, 873–883.